Flux vortex dynamics in type-II superconductors

J Srpčič[1], D A Moseley[1], F Perez[1], K Y Huang[1], Y Shi[1], A R Dennis[1], M D Ainslie[1], A M Campbell[1], M Boll[2], D A Cardwell[1] and J H Durrell[1]

[1]Engineering Department, University of Cambridge, Trumpington Street, Cambridge CB2 1PZ, UK

[2]Siemens AG Corporate Technology eAircraft, Willy-Messerschmitt-Str. 1, D-82024, Taufkirchen, Germany

E-mail: js2308@cam.ac.uk

September 2019

Abstract. The flux-pinning landscape in type-II superconductors determines the response of the flux line lattice to changing magnetic fields. Typically, the flux vortex behaviour is hysteretic and well described within the framework of the Bean critical-state model and its extensions. However, if the changing magnetic field does not move the flux vortices from their pinning sites, their response remains linear and reversible. The vortex displacement, then, is characterised by the Campbell penetration depth, which itself is related directly to the effective size of the pinning potential. Here, we present measurements of the Campbell penetration depth (and the effective size of the pinning potential) as a function of magnetic field in a single-grain bulk $GdBa_2Cu_3O_{7-\delta}$ superconductor using a pick-up coil method. Hence, the hysteretic losses, which take into account the reversible vortex movement, are established.

1. Introduction

The critical-state model proposed by Bean [1] represents the foundational framework which has been used to predict successfully most macroscopic observables of hard type-II superconductors in the mixed state. The simple assumptions that a) there exists an upper limit to the current density that can flow through the superconductor, called the critical current density, J_C, and b) any electromotive force will induce the full critical current density to flow, are sufficient to describe qualitatively the hysteretic behaviour of these materials. Furthermore, excellent quantitative agreement with experiment is achieved by taking into account the dependence of J_C on magnetic field [2] (J_C is assumed constant in Bean's original formulation).

The Bean model is phenomenological and purely macroscopic as it describes the behaviour of the mixed state, an ensemble of coupled flux vortices, by introducing the critical current density as an average over the current contribution of many individual vortices. All the vortices are assumed pinned in place – by pinning centres, essentially

potential wells – and will become unpinned in the presence of any electromotive force, regardless of its magnitude. In reality, however, a sufficiently small force, acting on a pinned vortex, will not displace the vortex from its potential well; instead the vortex will move from its equilibrium position within the potential well itself, and will return to equilibrium once the force is removed. This movement within the potential well is reversible and is neglected within the Bean model framework.

Campbell [3, 4] proposed an extension to the Bean model in the case of small applied magnetic fields, such that the vortices in the mixed state do not establish the critical state immediately after the applied field is turned on. Instead, the vortices initially move reversibly within their potential wells. The pinning force, which is assumed constant in the Bean model, is assumed linear in the Campbell model for small displacements (Hooke's law). If d is the maximum distance the vortices can move reversibly from their equilibrium positions (i. e. the effective size of the pinning potential), and y is the vortex displacement from equilibrium (Figure 1), the pinning force is assumed linear for $y \ll d$, and constant for $y \gg d$. The mixed state can, then, be viewed as an ensemble of coupled linear harmonic oscillators. Hence, small external applied magnetic fields can be shown to decay exponentially with distance in the superconductor (in contrast with the linear decay in the constant-J_C Bean model). The characteristic distance, over which the magnetic field decays, is the Campbell penetration depth, λ_C, and is determined by the size of the pinning potential, d (see the derivation, below).

In this paper we present a simple method of measuring the Campbell penetration depth and, with it, the effective size of the pinning centres, based on Campbell's original pick-up method. Originally, Campbell measured the AC response of the mixed state using a pick-up coil wound round a long and thin superconducting sample. The method entails applying a DC magnetic field to establish the mixed state, after which a superposed AC magnetic field is swept in amplitude and this allows the value of penetration at the applied DC magnetic field to be extracted from the pick-up voltage. This measurement is repeated for varying values of DC field to obtain the penetration profile of the applied field. Here, we simplify the method by showing that the slope of the pick-up voltage, as it passes zero, is directly determined by the value of λ_C (hence, making data analysis straightforward).

Typically, measurements of the Campbell penetration depth have been used to establish the magnetic field profiles for small applied magnetic fields in order to probe the current density profile close to the superconductor surface [5]. Additionally, as the value of λ_C will be determined by the pinning centre size, d, the method can be used to establish the effective size and dependence on DC magnetic field of the pinning potential [6]. Hence, a closely related quantity, the Labusch parameter [7], which is the effective curvature of the pinning potential, can be determined.

On the theoretical side, Brandt [8] analysed the mixed state near the superconductor surface using real and image vortices, and has shown that the (complex) AC penetration depth generally can be written as the sum of the Campbell and London penetration depths, $\lambda_{ac}^2 = \lambda_C^2 + \lambda_L^2$, transitioning from the former to the latter as $d \to 0$.

More recently, the Campbell model was analysed within the strong pinning framework by Willa et al. [9, 10], who demonstrated a "flux pumping" effect, whereby the flux in the superconductor will approach the external DC magnetic field value as a consequence of the superposed AC magnetic field.

In this work, we apply the Campbell framework to bulk high-temperature superconductors. These materials, in particular $YBa_2Cu_3O_{7-\delta}$ and $GdBa_2Cu_3O_{7-\delta}$, are interesting for applications requiring compact high magnetic fields [11]. Specifically, permanent-magnet-type rotating machines appear a likely candidate application in which bulk superconductors may be employed in the future [12]. In these applications the magnetic field environment of the superconductor will likely be a large DC magnetic field (due to the persistent currents in the material), and a comparatively smaller (in amplitude) AC magnetic field due to the non-ideal nature of the machine. This is precisely the regime in which the Campbell model becomes relevant (and in which the Bean model becomes less reliable).

In the following section the Campbell model is derived and the physical origin of the Campbell penetration depth is presented. Subsequently, the magnetic field profile inside the superconductor, the total flux and its time derivative (which is the induced voltage) are calculated. We show that, for sufficiently small amplitudes of AC magnetic field, the slope of the induced voltage signal at zero is determined by λ_C. In section 3 we present the measurement setup and in the final section we compare theory with experiment, which are shown to be in excellent agreement.

2. The magnetic field profile due to a linear pinning force

2.1. Derivation of the dynamic equations

In order to derive how a linear pinning force shapes the magnetic field profile in the superconductor, let us first consider how the local magnetic field changes due to a displacement of a flux vortex from its initial position (essentially leading to the flux conservation equation). The flux vortex distribution is shown schematically in Figure 1.

We begin with a superconductor above T_C and we apply a constant magnetic field, B_0. Subsequently, the temperature is lowered below T_C and the magnetic field B_0 is kept constant. This leads to a field-cooled mixed state in which the magnetic field density is constant throughout the superconductor, corresponding to a uniform flux vortex lattice, in which the vortices are parallel to B_0. Since each vortex contributes a flux quantum, Φ_0, to the total flux through the superconductor, the vortex spacing in one direction (e. g. the x-axis) can be expressed as

$$a = \frac{1}{w}\frac{\Phi_0}{B_0}, \tag{1}$$

where w is the vortex spacing perpendicular to the x-axis. In a uniform square vortex lattice $w = a$; however, we assign separate symbols because in the subsequent discussion the value of a will be made to change, whereas w will remain constant.
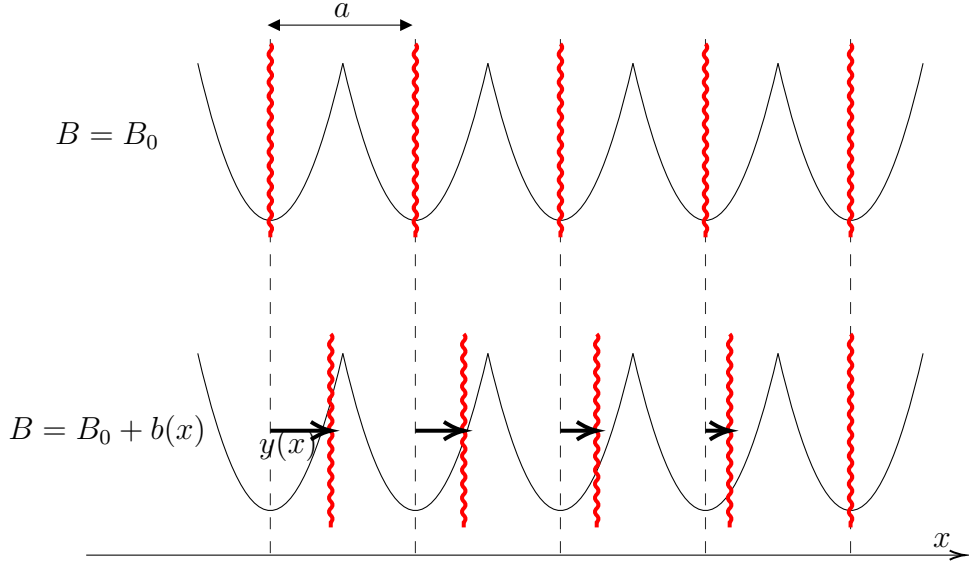
Figure 1. Top: a constant distribution of pinned flux vortices (red wavy lines) corresponds to a constant magnetic field B_0. The black lines represent the pinning centres as uniformly spaced harmonic potential wells. Bottom: a vortex displacement $y(x)$ from its equilibrium position in the pinning potential leads to a local change in magnetic field, $b(x)$. This image is valid for induced currents $J < J_C$. The vortex density gradient at $J = J_C$ is discussed later.

If the vortices are moved from their initial positions along x by some displacement, y, which may be a function of x, the new spacing can be written as

$$a_2 = a + y(x + a) - y(x). \tag{2}$$

This expression can be approximated with a derivative (provided the scale over which $y(x)$ changes is much greater than a) as

$$a_2 = a\left(1 + \frac{dy}{dx}\right). \tag{3}$$

Then, the new magnetic field at position x can be written as

$$B_2 = \frac{\Phi_0}{w\,a_2} = \frac{\Phi_0}{w}\frac{1}{a\,(1 + dy/dx)} \approx \frac{\Phi_0}{wa}\left(1 - \frac{dy}{dx}\right) = B_0\left(1 - \frac{dy}{dx}\right), \tag{4}$$

where we assumed $dy/dx \ll 1$. Hence, the change in field, $\Delta B = B_2 - B_0$, can be written as

$$\frac{\Delta B(x)}{B_0} = -\frac{dy}{dx}. \tag{5}$$

This is the flux conservation equation, which states that the change in field is directly proportional to the local change in vortex spacing. It is the first in a system of two coupled linear differential equations used to calculate the magnetic field profile in the superconductor.

The second differential equation will determine how $y(x)$, the vortex displacement, changes when an AC magnetic field is applied depending on what shape of pinning force

is assumed. As with the Bean model we start with the force balance equation for a single vortex

$$F_P = F_L, \tag{6}$$

where F_P is the pinning force and F_L the Lorentz force. Here, the thermal activation force and the vortex viscosity are neglected (in general the above equation is derived from the Langevin equation for vortex movement, see [13]). If we assume a constant pinning force, $F_P = B_0 J_C$, the subsequent derivation gives the Bean model equation, where the magnetic field profile in the superconductor has a constant slope, determined by the value of J_C:

$$\frac{dB}{dx} = \pm \mu_0 J_C, \tag{7}$$

where μ_0 is the permeability of free space.

Conversely, the Campbell model assumes a linear restoring force for small vortex displacements $y \ll d$ (d is the radius of the pinning potential), and a constant frictional force for $y \gg d$. Hence, a candidate pinning force may be

$$F_P(y(x)) = B_0 J_C \left(1 - \exp\left(-\frac{y(x)}{d} \right) \right). \tag{8}$$

The above dependence is appropriate as it is linear for $y \ll d$ and constant for $y \gg d$ (for $y \ll d$ the exponential part is approximated by $1 - y/d$, and for $y \gg d$ the exponential part is zero, as in the Bean model). Next, the Lorentz force can be written in terms of the local current density $J(x)$ as

$$F_L(x) = B_0 J(x) = B_0 \left(-\frac{1}{\mu_0} \frac{db(x)}{dx} \right), \tag{9}$$

where the current density is proportional to the local magnetic field gradient as per Ampere's law. We defined $b(x)$ as the local magnetic field due to the change in vortex spacing: the total magnetic field will be $B = B_0 + b(x)$. As B_0 is constant the field gradient in the above equation is simply $db(x)/dx$. The lower-case choice for b is to emphasise that $b \ll B_0$ throughout this work.

Inserting equations 8 and 9 into the force balance equation, and combining with the flux conservation equation 5 (in which we assume $\Delta B(x) = b(x)$) leads to the system of two first-order ordinary differential equations for vortex displacement $y(x)$ and the local magnetic field $b(x)$:

$$\frac{dy(x)}{dx} = -\frac{b(x)}{B_0}, \tag{10}$$

$$\frac{db(x)}{dx} = \mu_0 J_C \left(1 - \exp\left(-\frac{y(x)}{d} \right) \right). \tag{11}$$

The above equations can be solved numerically with an appropriate set of boundary conditions. For example, if the superconductor is an infinite slab occupying the space $-x_0 \leq x \leq x_0$ the solution will be symmetrical with respect to $x = 0$ and the boundary conditions will take the form $y(x = 0) = 0$ and $b(x = x_0) = b(x = -x_0) = B_{AC}$. Here,

the displacement is zero in the centre because of symmetry and the magnetic field at the surface is equal to the applied AC magnetic field, B_{AC}. In an infinite cylinder along the z-axis with radius ρ_0 the above equations can be modified by substituting $x \to \rho$ (ρ is the radial coordinate). Then the boundary conditions become $y(\rho = 0) = 0$ and $b(\rho = \rho_0) = B_{AC}$.

2.2. The pinning force hysteresis

The pinning force dependence on vortex displacement, as defined in equation 8, is only valid in describing the vortex behaviour insofar as the direction of change of the external field is not reversed (i. e. only in the first quarter period of the applied AC magnetic field). As such, the shape of the force-displacement dependence must be amended to account for hysteresis. In the case of the Bean model, for example, the local pinning force jumps from $F_P = B_0 J_C$ to $F_P = -B_0 J_C$ immediately upon the reversal of the applied field (Figure 2, grey arrows). Conversely, in the Campbell model the vortices must move a finite distance within their potential wells before re-establishing the critical state, meaning that the transition from the maximum to the minimum force will not be immediate.

In order to account for hysteresis it is assumed that the pinning force response at the reversal of the applied magnetic field is linear with displacement in the same way as when the magnetic field is first turned on. This is because the response of pinned vortices will be determined by the effective curvature of the pinning potential (similar to, for example, a linear harmonic oscillator for which the spring constant is the gradient of the potential). For this reason the hysteretic pinning force will be of a similar shape as in equation 8, except it will be scaled in both axes by a factor of 2 as its value must go from $B_0 J_C$ to $-B_0 J_C$ when the displacement goes from its maximum to its minimum value. Hence, if y_0 is the maximum vortex displacement during one period of AC field, the hysteretic pinning force can be written in terms of the initial pinning force as

$$F_P^{\pm}(y(x)) = \pm \left[2F_P \left(\frac{y_0 \pm y(x)}{2} \right) - F_P(y_0) \right], \tag{12}$$

which is shown schematically in Figure 2 (red arrows). The positive and negative sign correspond, respectively, to the increasing and decreasing segments of the hysteresis loop.

Once the total pinning force dependence on displacement is established the hysteretic losses per vortex can be calculated as the area of the loop. As a point of reference the Bean model will predict losses in the form

$$Q_B = 4B_0 J_C y_0, \tag{13}$$

which is simply the area of a rectangle with sides $2B_0 J_C$ and $2y_0$ (as shown in grey in Figure 2). The losses in the Campbell model will be given by the integral of the
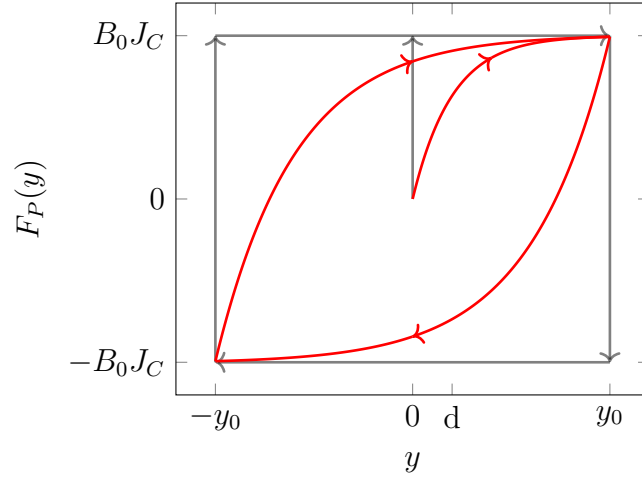
Figure 2. The pinning force hysteresis in the Campbell model (red line). The initial curve is $F_P(y)$ from equation 8. The two loop curves are $2F_P((y_0 + y)/2) - F_P(y_0)$ (top) and $-(F_P((y_0 - y)/2) - F_P(y_0))$ (bottom). The slope at $y = 0$ is the same as at $y = y_0$, and is determined by the curvature of the pinning potential. The Bean model force hysteresis is shown in grey.

hysteretic force as

$$Q_C = 2 \int_{-y_0}^{y_0} F_P^+(y) \, dy. \tag{14}$$

Evaluating the integral gives the ratio between the Bean and Campbell losses as

$$\frac{Q_C}{Q_B} = 2\frac{d}{y_0} \left(\exp\left(-\frac{y_0}{d}\right) - 1 \right) + \left(\exp\left(-\frac{y_0}{d}\right) + 1 \right). \tag{15}$$

At small maximum displacements $y_0 \ll d$, which is when the vortices behave as linear harmonic oscillators within the pinning centres, the losses can be shown to increase quadratically with displacement, i. e.

$$\frac{Q_C}{Q_B} \to \frac{1}{6}\frac{y_0^2}{d^2}, \tag{16}$$

and at large displacements, $y_0 \gg d$, at which the Campbell model approaches the Bean model, the losses become equivalent,

$$\frac{Q_C}{Q_B} \to 1. \tag{17}$$

2.3. The solutions of the dynamic equations

Once the hysteretic pinning force is established equations 10 and 11 can be solved by numerical integration to obtain the magnetic field profile $b(x)$ inside the superconductor caused by an external AC magnetic field. Since the equations are stationary they must be solved for boundary conditions which are themselves evolving in time in order to generate
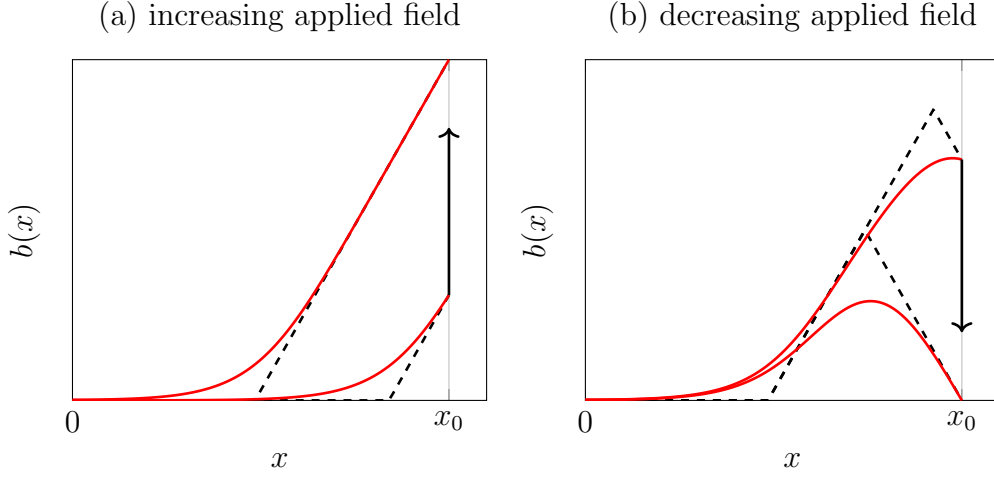
Figure 3. The Campbell (red) and Bean (black, dashed) magnetic field profiles during the (a) increasing and (b) decreasing portion of the applied field. $x = 0$ is the centre of the superconductor and $x = x_0$ is the surface. The black arrow represents the direction of change of the applied magnetic field.

a time dependence of $b(x)$. Specifically, the boundary condition at the superconductor surface will be

$$b(x = x_0) = B_{AC} \cos(\omega t), \tag{18}$$

where B_{AC} and ω are the amplitude and angular frequency of the AC field, respectively. The solution for $b(x)$ at different times, compared to the Bean model, is shown in Figure 3. The solution is for an infinite slab occupying the space $-x_0 \leq x \leq x_0$ (only $x > 0$ is shown due to symmetry). The solution for a cylinder of radius ρ_0 is equivalent with the substitution $x \rightarrow \rho$ and $x_0 \rightarrow \rho_0$.

Firstly, looking at the Bean model magnetic field profiles (black dashed line), the slope of $b(x)$ is constant and is, per equation 7, determined by the value of J_C. The transition from the positive to the negative slope (after the external field is reversed) is immediate because the flux vortices are assumed to establish immediately the critical state with the current in the opposite direction.

In the Campbell model (red lines) this will not be the case as the vortices initially move reversibly a finite distance (determined by the pinning potential size, d) before establishing the critical state with the current in the opposite direction. The consequence is that the cusp of the field profile gets smoothed, leading to a more realistic area of a finite size in which the current density can transition from $+J_C$ to $-J_C$. Additionally, the penetration in the Campbell model will be larger than in the Bean model because in the former the current density is allowed to transition smoothly from J_C to zero instead of a step function in the latter. Consequently, the shielding ability in the transition region will be decreased as well, leading to increased penetration.

The magnitude of the increased penetration is determined by λ_C, the Campbell penetration depth, which itself is determined by the size of the pinning centres, d, or

the maximum distance the vortices can move reversibly before becoming unpinned. To derive and expression for λ_C we assume the amplitude of the external AC magnetic field is sufficiently small so as not to unpin any vortices from their pinning centres. Consequently, the pinning force may be assumed linear,

$$F_P = B_0 J_C \frac{y}{d}, \tag{19}$$

and all the vortices may be treated as linear harmonic oscillators, and their movement reversible. In essence, this means that when the external magnetic field changes the flux vortex closest to the surface moves within its potential well, thereby shielding partially the interior of the superconductor (as in Figure 1). This is equivalent to a reversible shielding current being induced below the superconductor surface. Hence, the local magnetic field change felt by the adjacent vortex deeper in the superconductor interior will be lower and its displacement will be lower. This displacement will, in turn, further partially shield the interior and the next vortex will be displaced even less (and so on). By inserting the linear pinning force into the system of differential equations 10 and 11 it can be shown that the vortex displacement decays exponentially with distance,

$$y(x) \propto b(x) \propto \exp\left(-\frac{x}{\lambda_C}\right), \tag{20}$$

where

$$\lambda_C = \sqrt{\frac{B_0 d}{\mu_0 J_C}}. \tag{21}$$

The value of λ_C at a given DC magnetic field, B_0, and a given critical current density, J_C, will be determined by the size of the pinning centres, d. Hence, by measuring λ_C via the measurement of field profiles inside the superconductor we can probe the effective pinning potential size in the material.

2.4. The total magnetic flux and induced voltage in the Campbell model

The magnetic field profile $b(x)$, given by the Campbell model, can be integrated over the cross-section of the superconductor, giving the total magnet flux in the superconductor, Φ_m. Its time derivative, the induced voltage, is an easily measurable quantity using a pick-up coil wound round the superconductor. Hence, it is of interest to derive an expression connecting the shape of the induced voltage signal, and the value of λ_C.

In the Bean model the magnetic flux time dependence, $\Phi_B(t)$, can be calculated analytically by integrating the field profile $b(x)$ from Figure 3 over the cross-section of the superconductor. Assuming a long and thin superconductor with a square cross-section with a side length $2x_0$ the total flux can be calculated as

$$\Phi_B(t) = \int b(x)\, dS = 8x_0 \int_0^{x_0} b(x)\, dx, \tag{22}$$

where $8x_0$ is the circumference of the superconductor. This expression is true if $b(x)$ is non-zero only very close to the surface of the superconductor, which will be the case for
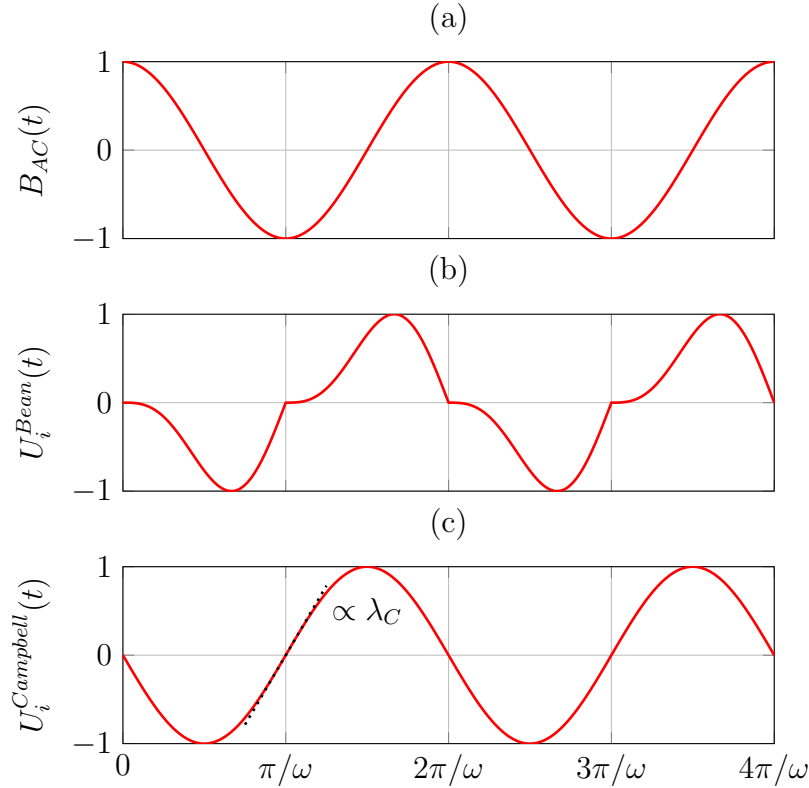
Figure 4. (a) The (normalised) applied magnetic field waveform, $B_{AC}(t)$, which induces a time dependent magnetic flux in the superconductor. The time derivative of the flux is the induced voltage and is shown in (b) for the Bean model and in (c) for the Campbell model. In the Campbell model the slope of the induced voltage at zero is determined by the Campbell penetration depth, λ_C (as indicated by the black dotted line).

small applied AC magnetic fields. Then, the integral will be non-zero only in a narrow strip close to the surface with an area $dS = 8x_0\, dx$, leading to the above result.

If the AC magnetic field is $B_{AC}(t) = B_{AC} \cos\omega t$, the solution is analytical, i. e.

$$\Phi_B(t) = \frac{2x_0 B_{AC}^2}{\mu_0 J_C} \left(1 + 2\cos\omega t - \cos^2\omega t\right). \tag{23}$$

The solution is valid in the range $0 \leq t < \pi/\omega$, after which it changes sign every half-cycle of the AC field. Its time derivative, the induced voltage, is shown in Figure 4 (b). In the moment following the peak applied field only the field profile close to the superconductor surface, $x = x_0$, will be affected (as shown in Figure 3 (b), black dashed lines). Consequently, the change in flux will be zero immediately following the reversal of applied field. Conversely, in the moment preceding the peak applied field the affected area will be close to maximum, up to the Bean penetration depth of the full applied field amplitude. The rate of change of flux will be determined by the rate of change of the applied field. For this reason there is a cusp in the induced voltage signal at each half-period of the applied field.

In the Campbell model the flux is calculated by substituting $b(x)$ in equation 22 by the solution of equations 10 and 11. Since the antiderivative of $b(x)$ is given by the flux conservation equation 11 the flux can further be written as

$$\Phi_C(t) = -8x_0 B_0 \left(y\left(x_0\right) - y\left(0\right) \right), \tag{24}$$

where $y(0) = 0$ due to the boundary condition, B_0 is the DC magnetic field, and $y(x_0)$ is the vortex displacement at the edge of the superconductor. The value of $y(x_0)$ can be obtained by solving the dynamic equations for $y(x)$ numerically and evaluating the solution at $x = x_0$. The resultant induced voltage, the time derivative of the flux, is shown in Figure 4 (c). After the applied field is reversed the penetration in the Campbell model is not limited to as narrow a region as it is in the Bean model and the transition in the slope of $b(x)$ is not immediate (as can be seen in Figure 3 (b), red lines). Consequently, the induced voltage waveform will be smoothed (as compared to the Bean model) and will approach a pure sine wave at low amplitudes of applied AC magnetic field, at which all vortex movement will be reversible.

For the purposes of data analysis it is desirable to derive an analytical expression describing the shape of the induced voltage, which would subsequently allow for a straightforward comparison between theory and experiment. Here, we show that by linearising the differential equations 10 and 11 we obtain an analytical expression for the slope of the induced voltage at zero (black dotted line in Figure 4 (c)).

The time, at which the induced voltage passes zero, is when the applied field is at its maximum amplitude. Hence, this corresponds to the maximum vortex displacement and the maximum pinning force (represented by the point $P = (y_0, F_0)$ in Figure 5). The tangent to the hysteretic pinning force $F_P^-(y)$ at P can be written as

$$F_{Linear} = B_0 J_C \left(\frac{y - y_0}{d} \right) + F_0, \tag{25}$$

where $F_0 = F_P(y_0)$. Substituting this expression into the differential equations 11 and 10 leads to a second order partial differential equation, which has the analytical solution

$$y(x) = \left(y_0 - \frac{F_0 d}{B_0 J_C} \right) \left(1 - \cosh \frac{x - x_0}{\lambda_C} \cosh^{-1} \frac{x_0}{\lambda_C} \right) - \lambda_C \frac{B_{AC}(t)}{B_0} \sinh \frac{x}{\lambda_C} \cosh^{-1} \frac{x_0}{\lambda_C}. \tag{26}$$

This solution can be inserted subsequently into equation 24, the time derivative of which gives the induced voltage simply as

$$U_i = 8x_0 \lambda_C \frac{\partial}{\partial t} B_{AC}(t), \tag{27}$$

which expression is valid when the voltage passes zero. This result can be compared to the induced voltage in the normal state (in which there is no shielding and the penetration is full), i. e.

$$U_i^N = -4x_0^2 \frac{\partial}{\partial t} B_{AC}(t), \tag{28}$$

where $4x_0^2$ is the cross section of the superconductor. The ratio of the two voltages is

$$\frac{|U_i|}{|U_i^N|} = 2\frac{\lambda_C}{x_0}. \tag{29}$$
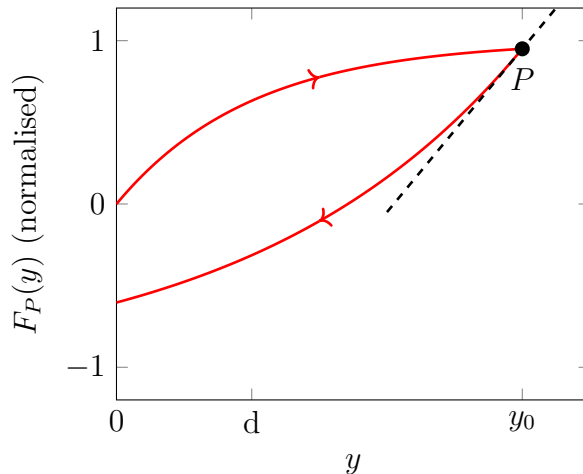
Figure 5. The pinning force at $y = y_0$ is approximated by a linear function.

By measuring the induced voltage in the superconducting state and in the normal state (at the same frequency and amplitude of the applied AC magnetic field), the Campbell penetration depth can be extracted from the ratio of the two measurements.

3. Experimental

All measurements were performed on a single grain $GdBa_2Cu_3O_{7-\delta}$ bulk superconductor, grown by the top-seeded melt growth technique [14, 15]. The sample was initially grown in a standard 30 mm diameter and 10 mm thick bulk, which was subsequently cut into a rectangular shape 5 mm by 5 mm by 10 mm, where the longest dimension is along the c-axis of the sample. The sample height-to-width ratio is only 2, whereas the derivation of the theoretical framework assumes an infinitely long sample. Due to the finite size of the sample the magnetic field lines at the top and bottom edges will bend, causing an increased penetration and, hence, a higher measured induced voltage. This means that our measurement might overestimate the values of λ. However, since the pick-up coil is wound along the height of the sample (see below) the measurement will give the value of λ, averaged over the sample height. This means that, while the value of λ increases close to the bottom and top edges of the sample, its contribution to the induced signal may not be significant since it will be averaged with the values of λ form the middle height of the sample.

The experimental set-up is shown in Figure 6. A pick-up coil of approximately 1000 turns was wound tightly round the sample and was used to measure the changing flux in the superconductor. The sample with the pick-up coil was inserted into a bore of a larger solenoid coil, which itself was used to generate an AC magnetic field by passing an alternating current through it. The current was set at 300 Hz and was adjusted so that the amplitude of the generated AC magnetic field was 1 mT at the sample (the coil current-field characteristic was measured using calibrated Hall sensors). The AC

coil with the sample was finally inserted into a bore of a large superconducting magnet, which was used to generate a DC magnetic field from 0.5 T to 6 T in amplitude. The temperature of the sample was kept constant at 70 K by means of helium gas in the variable temperature insert in the DC magnet.

The circuit diagram for the measurement consisted of two balancing rigs connected in series with the measurement pick-up coil. The first balancing rig (No. 1 in Figure 6) was a variable mutual inductance between the driving circuit and the pick-up circuit. The balancing rig was used for the purposes of subtracting the pick-up voltage due to the finite thickness of the pick-up coil. Since not all the wire, making up the pick-up coil, was directly in contact with the superconductor surface, a portion of the induced voltage would come from the AC magnetic field penetrating through the inner layers of the coil and inducing a voltage in the outer layers. This induced voltage had to be subtracted from the measurement since it held no information about the changing flux in the superconductor. The means by which this part of the signal was subtracted from the measurement was the AC magnetic field was initially applied to the superconductor in the Meissner state, when the DC magnetic field is zero (only the AC magnetic field was applied). The mutual inductance was tuned such that the measured induced voltage was zero. It follows, then, that any further signal acquired when the DC magnetic field was turned on was a measure of the field penetration beyond the London penetration depth.

The second balancing rig of the circuit (No. 2 in Figure 6) was a set of two mutual inductances, connected with a variable resistor. If the first balancing rig was used to subtract the signal in-phase with the induced voltage in the normal state, the second balancing rig was used to subtract a signal component 90 degrees out-of-phase. If there are any poorly made connections in the circuit there will be parasitic capacitances present, which will shift the signal by one quarter period. Similarly, if there are any conductors present in which eddy currents can be induced the back emf from the eddy currents will induce a phase shifted signal in the pick-up coil. For this reason the second balancing rig was used to subtract any out-of-phase signal from the measurement. The balancing in both cases was done at zero DC magnetic field before the measurements took place. By this balancing mechanism the signal could be balanced to 0.1%. Additionally, the signal-to-noise ratio was further improved by averaging the signal over 1000 periods of the applied AC field. Finally, the signal was passed through an amplifier with a band gap filter and acquired by a data acquisition card.

4. Results

The induced voltage was measured for varying values of DC magnetic field, at a fixed applied AC magnetic field of amplitude 1 mT and frequency 300 Hz. The measured voltage waveforms are shown in Figure 7.

All the measured waveforms in their raw form were shifted in phase by a DC-field-dependent value, which indicates losses due to flux flow viscosity [16]. Here, this
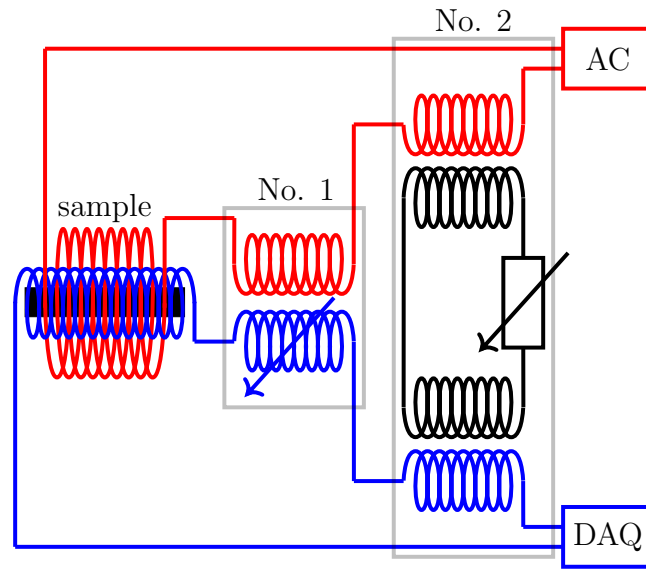
Figure 6. The circuit diagram of the measurement set-up (in red is the driving AC coil, in blue the pick-up circuit connected to the data acquisition card). The sample with the two enveloping coils is inserted into a superconducting DC magnet (not shown). The two balancing rigs are labelled No. 1 and No. 2.
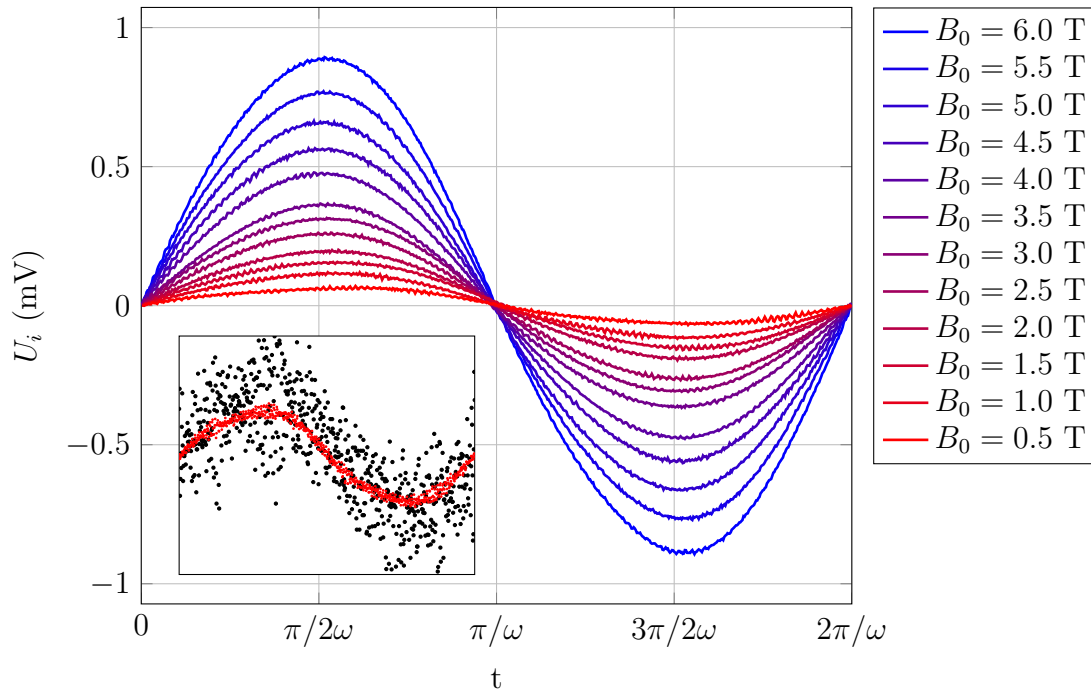

Figure 7. The induced voltage signal at the AC magnetic field amplitude 1 mT and frequency 300 Hz, at varying DC magnetic fields. The inset shows a comparison between the raw data (black dots) and the averaged signal for $B_0 = 0.5$ T.

phase shift was zeroed for the purposes of comparing the waveform shapes; however its value can be used in determining the magnitude of the viscous force as it appears in the Langevin equation of vortex motion. With the phase shift subtracted the waveforms can be seen – although slightly asymmetrical as in the case of the Bean waveform, Figure 4 (b) – to approach the pure sine wave as is the case when the vortex movement is reversible.

The slope of the voltage signal as it passes zero appears to increase with increasing applied DC magnetic field. Hence, by plotting the slope as a function of DC field the dependence of the value of λ_C can be extracted using equation 29. The results are shown in Figure 8.

The field dependence of the Campbell penetration depth is shown in Figure 8 (a). The scale is on the order of ≈ 50 μm, which means that our assumption in deriving the total flux in the superconductor (i. e. the penetration depth is much smaller than the radius of the sample) is justified. The scale is, however, orders of magnitude larger than the London penetration depth, which, in $YBa_2Cu_3O_{7-\delta}$, is on the order of $\lambda_{London} \approx 100$ nm [18]. Hence, the reversible magnetic field penetration in the Meissner state (when B_0 is zero) is limited to ≈ 100 nm, and increases two orders of magnitude in the mixed state, when there are flux vortices pinned in the superconductor.

Once the field dependence of λ_C is established the effective size of the pinning potential, d, can be calculated (provided the field dependence of the critical current density is known). The critical current density, shown in Figure 8 (b), was measured from a representative sample by measuring the width of the magnetisation hysteresis loops at various DC magnetic fields at 70 K (see e. g. [17]). Hence, the calculated values of d are shown in Figure 8.

The values of d appear to be lower at the extremes of the measured magnetic field range, with a maximum at about $B_0 = 3$ T. This is because at low values of B_0 the pinning force, holding the vortices in place, will be high; the strong pinning will impede vortex movement, hence the effective size of the pinning potential will be low. Conversely, at high values of B_0 the vortex pinning force will be low, but the vortex density will be high. For this reason the vortex-vortex interactions will impede vortex movement and the effective pinning size will, again, be low. In contrast, at intermediate values of B_0 there will be a trade-off between the two effects, leading to a maximum in the size of the pinning potential.

As a point of reference for the scale of d, the vortex spacing as a function of B_0 for an ideal triangular lattice,

$$a(B_0) = \left(\frac{8}{3\sqrt{3}} \frac{\phi_0}{B_0} \right)^{\frac{1}{2}}, \tag{30}$$

where ϕ_0 is the flux quantum, is shown in Figure 8 (c) in red line. The values of d at high magnetic fields appear much lower than the values of a, which is not an intuitive result, since at high fields inter-vortex interactions will dominate. A possible explanation for this discrepancy is the sensitivity of our method to the accurate measurement of the
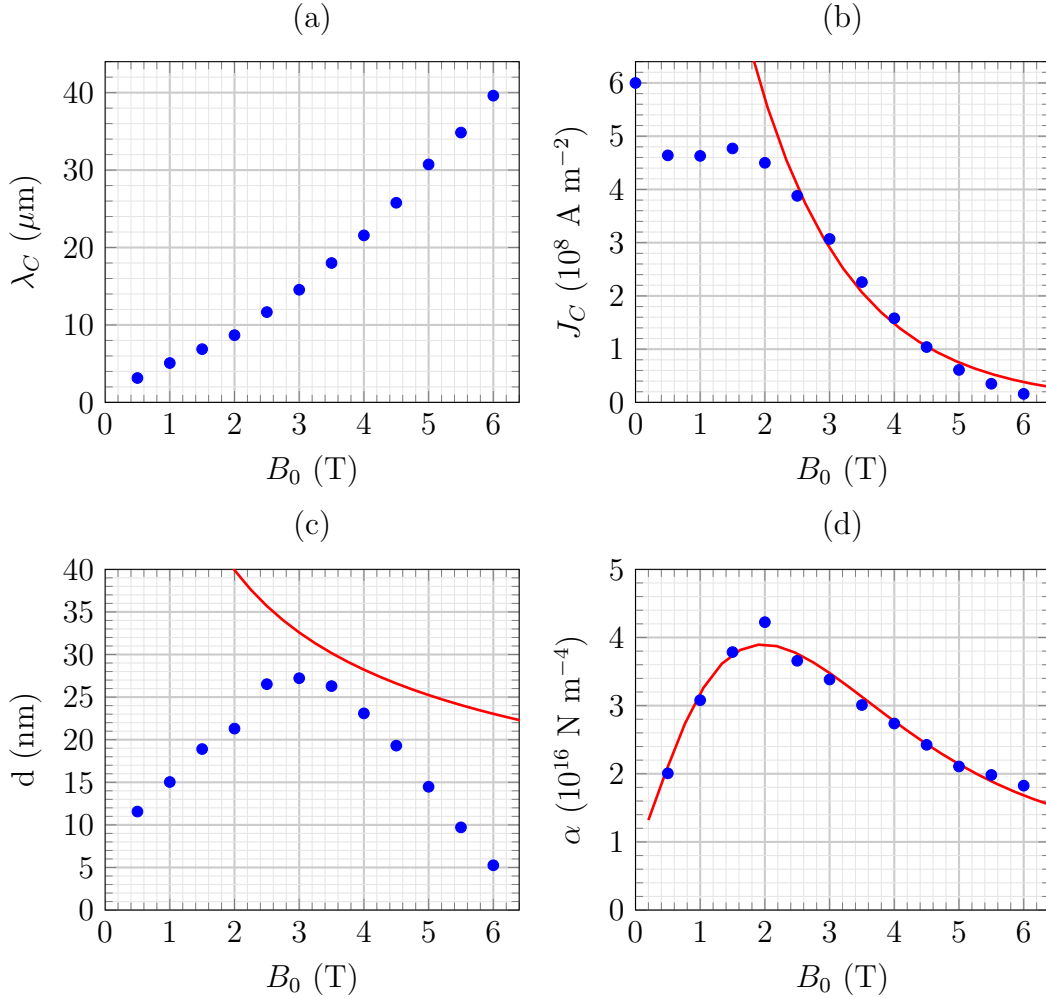
Figure 8. (a) The values of the Campbell penetration depth at various DC magnetic field values, as extracted from the induced voltage data. (b) The field dependence of the critical current density, measured from a representative bulk superconductor. The red line illustrates the exponential dependence of J_C on B_0 as would be the case in the absence of the peak effect (see text). (c) The effective size of the pinning potential, calculated from the λ_C values using equation 21. The red line, added as a point of reference, represents the vortex spacing in an ideal triangular lattice as a function of B_0.(d) The curvature of the pinning potential at its minimum, the Labusch parameter. The red line is a least square fit of the function $\alpha(B_0) = c_1 + c_2 B_0^{3/2} \exp{(-B_0/c_3)}$, where $c_1 = 0.95$ N m^{-4}, $c_2 = 4.76$ N m^{-4} T$^{-3/2}$, and $c_3 = 1.31$ T.

sample size. It is difficult to know the exact size of the superconducting material, contributing to the measured pick-up voltage, which might present a source of error for the absolute values of λ and d. However, in the scope of the present paper it is of interest mainly to measure the dependence of the Campbell parameters on magnetic fields, not necessarily their absolute values. It is also worth remembering that the value of d represents the maximum reversible displacement of the vortices from their equilibrium positions, but the transition is not immediate due to the choice of the pinning force

8. Hence, a lower value of d simply means that the vortices enter into the irreversible regime more quickly regardless of what the inter-vortex interaction may be.

The field dependence of the Campbell penetration depth, λ_C, and of the effective pinning potential size, d, appear in agreement with the data reported in [6] for samples with high densities of pinning centres. This is to be expected as the nature of the top-seeded melt growth leads to a high concentration of non-superconducting inclusions, which act as effective pinning centres.

Figure 8 (d) shows the field dependence of the effective curvature of the pinning potential at its minimum, the Labusch parameter, α [7]. Here, we use the definition of the maximum pinning force per unit volume per pinning diameter,

$$\alpha = \frac{B_0 J_C}{d}, \tag{31}$$

hence the units N m^{-4}. The value of α will depend on both the maximum pinning force at a given field, $B_0 J_C$, as well as on the size of the pinning potential, d. The peak in the value of α can be seen to correspond to the peak effect in the $J_C(B_0)$ dependence (around $B_0 = 2$ T) despite the values of d exhibiting a peak as well.

The shape of the $\alpha(B_0)$ dependence can be analysed by (for the moment) neglecting the peak effects in the $J_C(B_0)$ and $d(B_0)$ dependences. The $J_C(B_0)$ dependence in the absence of an observable peak effect is often approximated by an exponential function [19], i. e.

$$J_C(B_0) \propto \exp\left(-B_0/B_1\right), \tag{32}$$

where B_1 is some constant (red line in Figure 8(b)). Similarly, a reasonable approximation for the effective pinning size will be as some fraction of the inter-vortex spacing a (provided the inter-vortex interaction is the dominating force in the system, as will likely be the case at high magnetic fields). Hence,

$$d(B_0) \propto a(B_0) \propto B_0^{-1/2}, \tag{33}$$

where $a(B_0)$ is the vortex spacing in an ideal triangular lattice (red line in Figure 8 (c)). Then, the Labusch parameter can be written as

$$\alpha = \frac{B_0 J_C}{d} \propto \frac{B_0 \exp\left(-B_0/B_1\right)}{B_0^{-1/2}} = B_0^{3/2} \exp\left(-B_0/B_1\right). \tag{34}$$

This result is shown in red in Figure 8 (d) and appears in good agreement with the measured data.

It is evident from Figure 8, however, that the measured values of d do not follow the $\propto B_0^{-1/2}$ dependence. We have shown that if the critical current density were purely exponential and the size of the pinning parameter $d \propto B_0^{-1/2}$, the equation 34 would suffice to describe accurately the field dependence of the Labusch parameter. Since the equation 34 still describes well the field dependence of the Labusch parameter, it can be assumed that the deviation of $J_C(B_0)$ from the purely exponential dependence is in some way correlated with the deviation of the value of d from the $\propto B_0^{-1/2}$ dependence.
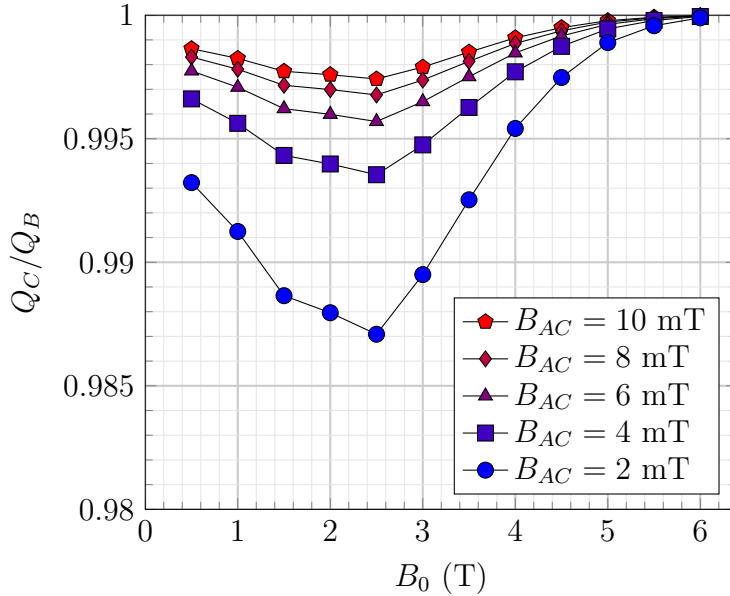
Figure 9. The ratio of the losses (per vortex per cycle) in the Campbell and in the Bean model as a function of magnetic field B_0, and at varying amplitudes of AC magnetic field.

In other words, it appears that the peak effect in $d(B_0)$ is correlated with the peak in the $J_C(B_0)$ dependence.

Once the size of the pinning potential is established the hysteretic losses per vortex can be obtained by integrating the force-displacement loop (Figure 2), the area of which corresponds to the losses generated during one cycle of applied AC magnetic field. As can be seen from equation 15 the ratio of the losses in the Bean and Campbell model will depend both on the maximum vortex displacement, y_0, and on the size of the pinning potential, the linear region d. For $y_0 \gg d$ the losses, predicted by the two models, will become equivalent (since the relative area of the linear region will go to zero). As an example, the maximum vortex displacement at the surface of the superconductor (at which the local magnetic field due to the applied AC magnetic field will oscillate with the highest amplitude) can be calculated via the flux conservation equation 11 by substituting the Bean model magnetic field profile 7. The solution is simply

$$y_0 = \frac{B_{AC}}{\mu_0 J_C}, \tag{35}$$

where the higher order term in B_{AC}/B_0 is neglected since $B_{AC} \ll B_0$. This can be substituted into equation 15 to calculate the losses given the measured values of d. The result is shown in Figure 9.

It is clear that the difference between the two models is small at the chosen amplitudes of AC magnetic field since the value of the maximum vortex displacement y_0 s much grater than the values of d at any value of B_0. For example, the highest difference between the two models is at $B_0 = 2.5$ T and $B_{AC} = 2$ mT (blue circles

in Figure 9). At that point $d = 26$ nm, whereas $y_0 = 4$ μm, a factor of ≈ 150 higher. Therefore the linear region in the hysteresis loop becomes negligible and the Bean model becomes sufficiently accurate. At lower amplitudes of AC magnetic field, however, the reversible vortex movement has to be taken into account.

5. Discussion

The data measured with our simplified method appear to be in good qualitative agreement with literature; however not every step in the derivation was explicitly justified. In particular, it is unclear why the slope of the pinning force hysteresis (Figure 2) is determined by the curvature of the pinning potential at its minimum. When the critical state is established there will be a density gradient of trapped flux vortices, determined by the depth of the pinning potential (the vortices will only just be pinned in place and will be at the very edge of the potential well). Then, if the applied field is reversed the density gradient will be established in the opposite direction, and the vortices will move from one edge of the pinning potential to the other before re-establishing the critical state. In such a situation the immediate response of the vortices will not be the same as in the virgin state. One possible explanation for this would be if the vortices are pinned on several point-like defects along their length, and the reversible movement that we observe is the movement of the parts of the vortex not pinned by the pinning centres - much like vibrations on a string.

The vortex viscosity, η, was neglected in our calculation for simplicity; however, all the voltage data were phase-shifted at varying values of magnetic field B_0, indicating a non zero vortex viscosity. If the force balance equation is modified to include η, i. e.

$$\eta \frac{\partial y}{\partial t} = F_L - F_P, \tag{36}$$

it can be shown that the Campbell penetration depth is generalised in the form

$$\lambda_C = \frac{B_0}{\sqrt{\alpha - i\omega\eta}}, \tag{37}$$

where i is the imaginary unit and ω is the AC magnetic field frequency. Then, the phase shift will be in the form

$$\Delta\phi = \arctan\frac{\omega\eta}{\alpha}, \tag{38}$$

from which the value of η can be extracted.

Finally, this method is sensitive to changes in sample geometry: if the sample cross-section is not constant all throughout its height the value of λ_C, given by equation 29, will change (i. e. the value of λ_C will be determined by the value of x_0 for a given voltage measurement). Hence, it is desirable to measure the sample size as precisely as possible in order to avoid systematic errors when determining the value of λ_C.

6. Conclusion

In this paper we presented a simplified method for measuring the effective size of the pinning potential in type-II superconducting materials, based on Campbell's original work [3]. We have shown that by measuring the shape (i. e. the slope at zero) of the induced voltage signal due to a changing flux in the superconductor of known dimensions, the pinning potential size, d, a quantity on the nanometre scale, can be observed. We presented measurements of d for a varying DC magnetic field and have shown the data agree with values reported in literature.

The measurements of d in various samples of type-II superconductor are useful as they provide insight into the governing mechanism of vortex pinning, as well as the size of pinning centres themselves. This is essential information aiding in the manufacture and development of high-quality superconducting materials with high current carrying capabilities. Additionally, since numerous possible future – and existing – applications of bulk superconducting materials entail a combination of a large DC and small ripple AC magnetic field, the Campbell model provides a useful framework within which the AC losses, induced in the superconductor, can be quantified and analysed more accurately than within the critical-state framework.

Acknowledgments

References

[1] C. P. Bean. *Magnetization of hard superconductors*. Physical Review Letters, 8(6):250, 1962.
[2] Y. B. Kim, C. F. Hempstead, A. R. Strnad. *Magnetization and critical supercurrents*. Physical Review, 129(2):528, 1963.
[3] A. M. Campbell. *The response of pinned flux vortices to low-frequency fields*. Journal of Physics C: Solid State Physics, 2(8):1492, 1969.
[4] A. M. Campbell. *The interaction distance between flux lines and pinning centres*. Journal of Physics C: Solid State Physics, 4(18):3186, 1971.
[5] R. W. Rollins, H. Küpfer, W. Gey. *Magnetic field profiles in type-II superconductors with pinning using a new ac technique*. Journal of Applied Physics, 45(12):5392, 1974.
[6] H. Küpfer, A. A. Zhukov, R. Kresse, R. Meier-Hirmer, W. Jahn, T. Wolf, T. Matsushita, K. Kimura, K. Salama. *Comparison of pinning parameters between low-T_C superconductors and $YBa_2Cu_3O_{7-\delta}$*. Physical Review B, 52(10):7689, 1995.
[7] R. Labusch. *Calculation of the critical field gradient in type-II superconductors*. Crystal Lattice Defects, 1:1-16, 1969.
[8] E. H. Brandt. *Penetration of magnetic ac fields into type-II superconductors*. Physical Review Letters, 67(16):2219, 1991.
[9] R. Willa, V. B. Geshkenbein, G. Blatter. *Campbell penetration in the critical state of type-II superconductors*. Physical Review B, 92:134501, 2015.

[10] R. Willa, V. B. Geshkenbein, G. Blatter. *Probing the pinning landscape in type-II superconductors via Campbell penetration depth.* Physical Review B, 93:064515, 2016.

[11] J. H. Durrell, A. R. Dennis, J. Jaroszynski, M. D. Ainslie, K. G. B. Palmer, Y. H. Shi, A. M. Campbell, J. Hull, M. Strasik, E. E. Hellstrom, D. A. Cardwell. *A trapped field of 17.6 T in melt-processed, bulk Gd-Ba-Cu-O reinforced with shrink-fit steel.* Superconductor Science and Technology, 27(8):082001, 2014.

[12] J. H. Durrell, M. D. Ainslie, D. Zhou, P. Vanderbemden, T. Bradshaw, S. Speller, M. Filipenko, D. A. Cardwell. *Bulk superconductors: a roadmap to applications.* Superconductor Science and Technology, 31(10):103501, 2018.

[13] V. A. Shklovskij, O. V. Dobrovolskiy. *ac-driven vortices and the Hall effect in a superconductor with a tilted washboard pinning potential.* Physical Review B, 78:104526, 2008.

[14] K. Sawano, M. Morita, M. Tanaka, T. Sasaki, K. Kimura, S. Takebayashi, M. Kimura, K. Miyamoto. *High magnetic flux trapping by melt-grown YBaCuO superconductors.* Japanese Journal of Applied Physics, 30(2):L1157, 1991.

[15] D. K. Namburi, Y. Shi, A. R. Dennis, J. H. Durrell, D. A. Cardwell. *A robust seeding technique for the growth of single grain (RE)BCO and (RE)BCO–Ag bulk superconductors.* Superconductor Science and Technology, 31(4):044003, 2018.

[16] Y. B. Kim, C. F. Hempstead, A. R. Strnad. *Flux-Flow Resistance in Type-II Superconductors.* Physical Review, 139(4A):A1163, 1965.

[17] M. D. Ainslie, H. Fujishiro, H. Mochizuki, K. Takahashi, Y. Shi, D. K. Namburi, J. Zou, D. Zhou, A. R. Dennis, D. A. Cardwell. *Enhanced trapped field performance of bulk high-temperature superconductors using split coil, pulsed field magnetization with an iron yoke.* Superconductor Science and Technology, 29(7):074003, 2016.

[18] T. Pereg-Barnea, P. J. Turner, R. Harris, G. K. Mullins, J. S. Bobowski, M. Raudsepp, R. Liang, D. A. Bonn, W. N. Hardy. *Absolute values of the London penetration depth in $YBa_2Cu_3O_{6+y}$ measured by zero field ESR spectroscopy on Gd doped single crystals.* Physical Review B, 69:184513, 2004.

[19] T. Kobayashi, T. Kimura, J. Shimoyama, K. Kishio, K. Kitazawa, K. Yamafuji.. *Exponential field dependence of critical current density of underdoped $(La_{1-x}Sr_x)_2CuO_4$ single crystals.* Physica C: Superconductivity, 254:213, 1995.